

MULTI-TENSOR FIELD SPECTRAL SEGMENTATION FOR WHITE MATTER FIBER BUNDLE CLASSIFICATION

Omar Ocegueda Mariano Rivera

Centro de Investigacion en Matematicas
Guanajuato, Gto, Mexico, 36240

ABSTRACT

We present an algorithm for segmenting the white-matter axon fiber bundles from HARDI images. We formulate the segmentation problem as a Multi-Tensor Field segmentation problem in which the compartments of each Multi-Tensor may belong to different classes, allowing the algorithm to handle crossing fiber tracts. Experimental results on two publicly available synthetic datasets and the fiber-cup phantom show that fiber crossings can be effectively separated by using this approach, and preliminary results on real data show that the segmentation obtained is consistent with known anatomical structures.

Index Terms— Brain imaging; Image segmentation; Tensor and vector field analysis

1. INTRODUCTION

Diffusion-Weighted Magnetic Resonance Imaging (DW-MRI) is a technique that allows us to study the anatomical structure of living tissues by quantifying the amount of water molecules that move along a set of M diffusion directions $Q = \{q_i\}_{i=1}^M$. When studying DW-MRI signals from the brain, it is possible to extract useful information related to the orientation of the axon fibers that pass through a given voxel, which can further be used to identify larger anatomical structures in the brain. The identification of anatomical structures of cerebral white matter from DW-MRI has been extensively studied in recent years by the neuroscience community with different objectives in mind [1–5]. Strategies for segmenting the white matter fiber bundles may be classified into two main categories: tractography-based clustering methods, and direct volume segmentation methods. Tractography-based clustering methods consist on generating a large set of trajectories (which is called tractography) that traverse areas of the brain with high diffusivity coherence. The set of trajectories are then grouped into clusters using a specific similarity metric, and the volume segmentation may be finally performed in terms of the number of classified trajectories that pass through each voxel, see for example Wassermann *et al.* [11].

Most direct volume segmentation methods formulate the problem as a binary segmentation problem, in which the bundle of interest (foreground) is separated from the rest of the volume (background), thus requiring a good initialization. Lankton *et al.* [5] proposed an active-contour evolution algorithm that uses local statistics to model the foreground data, the bundle of interest is manually indicated by two endpoints which are then connected using tractography, the pathway is then dilated to initialize a level-set binary segmentation method. Descoteaux *et al.* [2] used the coefficients of the Spherical Harmonics representation of the diffusion Orientation Diffusion Functions (ODF) to compute a similarity measure between neighboring ODF's. Then they used level-sets to segment the volume into foreground-background. Çetingil *et al.* [1] use manifold learning techniques to learn a sparse representation of the ODF at each voxel. They then compute a similarity matrix between pairs of voxels using the coefficients of the ODF's sparse representations and apply spectral clustering. The main drawback of most direct segmentation methods is that the segmentation task is formulated at the voxel level: each voxel is classified into one of the classes. However, when two or more fibers cross at a voxel, it is necessary to assign such a voxel to different classes. Hagmann *et al.* [3], and Jonasson *et al.* [4] proposed to formulate the segmentation problem on an extended space, called *Position-Orientation Space* (POS). Under the POS model, the estimated ODF's across the volume may be regarded as a scalar function S from a discretization of $\mathbb{R}^3 \times \mathcal{S}^2$ to \mathbb{R} , where \mathcal{S}^2 is the unit 2-sphere in \mathbb{R}^3 . In POS, the classification task can be solved by binarizing the 5-dimensional image S (high intensity corresponds to the presence of a fiber while low intensity corresponds to background). The main drawback of POS is that the discretization of the 5-dimensional space produces huge hyper-volumes which is highly memory demanding.

Our contribution is the development of an automatic fiber bundle segmentation method with the following characteristics: (i) It does not rely on tractography, (ii) It does not require user initialization nor an anatomical atlas to guide the segmentation (iii) Despite the high dimensionality involved, it is computationally efficient.

2. MULTI-TENSOR FIELD REPRESENTATION OF THE DW-MRI DATA

The DW-MRI signal $F_v : Q \rightarrow \mathfrak{R}$ at each voxel $v \in \Omega$ may be represented as a vector $S_v \in \mathfrak{R}^M$, where Ω is the set of all scanned voxels, and the i^{th} element of S_v is $S_{v,i} = F_v(q_i)$, $1 \leq i \leq M$. One of the most widely used tools for modeling the DW-MRI signals is Diffusion Tensor Imaging (DTI), which models the input signal as a *diffusion function*:

$$S_{v,i} = S_0(v) \exp(-\tau q_i^T D_v q_i). \quad (1)$$

where $S_0(v)$ is the standard T2 image at voxel v , D_v is a symmetric positive definite tensor and τ is the effective diffusion time. The most important limitation of DTI is that it is unable to resolve axon fiber crossings. One of the most successful approaches developed to overcome the limitations of the DTI model is the Multi-Tensor (MT) Model developed by Tuch *et al.* [10]. Under the MT model, each one of the n_v axon fibers passing through a given voxel v produces a single diffusion function, as in eq. 1, and the observed signal S_v is represented as a positive linear combination of those diffusion functions:

$$S_{v,i} = S_0(v) \sum_{j=1}^{n_v} \beta_j^{(v)} \exp(-\tau q_i^T D_v^{(j)} q_i). \quad (2)$$

where the positive coefficients $\{\beta_j^{(v)}\}_{j=1}^{n_v}$ indicate the volume-fraction of the voxel v that is occupied by the corresponding fiber. If we denote by $I = \{1, 2, \dots, K\}$, where $K = \max\{n_v : v \in \Omega\}$, we can think of the set $\mathcal{C} = \Omega \times I$ of *compartments* as an extension of the volume Ω obtained by “splitting” each voxel v in K parts, and each non-empty compartment represents the presence of a fiber bundle passing through the corresponding voxel. In our experiments, we used the Diffusion Basis Functions Model (DBF) proposed by A. Ramírez *et al.* [8] to fit the multi-tensor model to the data. Under the DBF, a fixed dictionary of N possible diffusion functions is used for all voxels in the volume, so that the model can be fit to the data by solving a non-negative least squares problem:

$$\beta^* = \min_{\beta \in \mathfrak{R}^N} \|\Phi\beta - S_v\|_2^2, \quad s.t. \beta \geq 0, \quad (3)$$

where $\Phi = [\phi_1, \phi_2, \dots, \phi_N]$ is the dictionary of diffusion functions evaluated at the set Q of diffusion directions, and hence may be regarded as M -dimensional vectors. Each column ϕ_j is then characterized by one tensor D_j . The set of eigenvalues of D_j (which is known as the *diffusivity profile*) is assumed to be constant and of the form $\Lambda = (\lambda_L, \lambda_R, \lambda_R)$, where λ_R is the *radial diffusivity* and $\lambda_L > \lambda_R$ is the *longitudinal diffusivity*. Therefore, each column ϕ_j is totally characterized by Λ and the principal diffusion direction (PDD) p_j of D_j . The DBF model has been shown to be a trusty approach in recent comparative studies ¹.

¹<http://hardi.epfl.ch/static/events/2012.ISBI/>

3. MULTI-TENSOR FIELD SPECTRAL SEGMENTATION

Since, under the DBF model, the diffusivity profile is constant, the DBF representation of the input signal S_v (eq. 2) is totally characterized by the set of positive coefficients $\{\beta_j^{(v)}\}_{j=1}^{n_v}$, and the set of principal diffusion directions of the tensors $\{D_v^{(j)}\}_{j=1}^{n_v}$. After fitting the DBF model to all voxels of the volume, we obtain a Multi-Tensor Field (MTF), which may be regarded as a function $\mathcal{T} : \mathcal{C} \rightarrow \mathfrak{R}^3$, that assigns a scaled PDD (a vector in \mathfrak{R}^3) to each compartment where the length $\|\mathcal{T}(v, j)\| = \beta_j^{(v)}$ encodes the positive coefficient and the unit vector $\frac{\mathcal{T}(v, j)}{\|\mathcal{T}(v, j)\|}$ encodes the PDD corresponding to the j^{th} tensor in the DBF representation of the signal S_v at voxel v . This representation is also convenient to encode the empty compartments: $\mathcal{T}(v, j) = 0$ indicates that the compartment (v, j) is empty. A segmentation of the MTF can therefore be defined as a function $L : \mathcal{C} \rightarrow \mathcal{L}$ that assigns an element from a set of labels $\mathcal{L} = \{1, 2, \dots, \ell\}$ to each compartment $(v, j) \in \mathcal{C}$ in such a way that the MTF \mathcal{T} is homogeneous (in some sense) along regions of \mathcal{C} sharing the same label. The requirement that \mathcal{T} is homogeneous along regions of the same class, needs to be defined more precisely by defining a notion of proximity (or *neighborhood*) between elements of \mathcal{C} and a notion of similarity (or distance) between elements of the range of \mathcal{T} . In our representation, a fiber bundle is formed by a set of nearby tensors with locally coherent orientation, thus a reasonable similarity metric between elements in the range of \mathcal{T} should consider both, spatial proximity and orientation. We used the dissimilarity measure given by $D((v, r), (w, s)) = \frac{\|v-w\|^2}{d_0^2} + \frac{\angle(r, s)}{\theta_0}$, and the similarity measure given by $\mathcal{S}((v, r), (w, s)) = \exp(-D((v, r), (w, s)))$, where $d_0, \theta_0 > 0$ are constant parameters and $\angle(\cdot, \cdot)$ denotes the angle between the non-zero vectors given as argument.

Given two neighboring voxels $v, w \in \Omega$ we first compute the *best* assignment of compartments in v to compartments in w , by minimizing the sum of the dissimilarities between paired tensors. Only paired tensors may be neighbors of each other. We say two paired compartments $(v, i), (w, j) \in \mathcal{C}$ are neighbors if $\angle(r, s) < \theta_{max}$, where $r = \mathcal{T}((v, i))$, $s = \mathcal{T}((w, j))$ and $\theta_{max} \geq 0$ is a constant parameter. The main difficulty in the segmentation of the MTF is that there is no simple way of modeling the variation of \mathcal{T} (a vector field) along each class (a fiber bundle). Thus, instead of modeling such variations, we define a transformation (“embedding function”) $F : \mathcal{C} \rightarrow \mathfrak{R}^d$ for a fixed $d > 0$, such that tensors that are close to each other according to the above distance D are mapped to nearby points in \mathfrak{R}^d . This kind of transformation is used in several dimensionality reduction and perceptual grouping algorithms. We used the algorithm proposed by Meila and Shi [7], which consists of comput-

ing the d eigenvectors $\{z^{(1)}, z^{(2)}, \dots, z^{(d)}\}$ of the $n \times n$ similarity matrix corresponding to its d largest eigenvalues. The embedding of the i -th compartment is then computed as $(z_i^1, z_i^2, \dots, z_i^d) \in \mathbb{R}^d$. In our case, n is the number of non-empty compartments, which may be very large, however since each compartment is only connected to a subset of its neighbors in the volume lattice, the resulting similarity matrix is very sparse. Thus, it is possible to compute the required eigenvectors using efficient algorithms such as Arpack [6], which we used in our experiments.

After embedding the points in \mathbb{R}^d it is possible to apply any standard segmentation algorithm, since the models in the embedded space are constant vectors in \mathbb{R}^d . We initialized the segmentation with K-means, and then apply Entropy-Controlled Quadratic Markov Measure Field (EC-QMMF) [9] to obtain the final segmentation. EC-QMMF is suitable for parametric segmentation (*i.e.*, to compute both the segmentation and the model parameters, which in our case are constant vectors in \mathbb{R}^d), and provides for each data point, a discrete distribution indicating the probability of the given point to belong to each of the classes.

4. EXPERIMENTS

We performed experiments at three levels of difficulty. The objective of the first experiment is to show the segmentation obtained when the *true* MTF is known (thus, the MTF estimation is not required), this experiment was performed on the publicly available 2012 HARDI Reconstruction Challenge dataset¹. The second experiment was performed on the publicly available fibercup phantom². In this case the bundles can be visually identified, but the MTF must be estimated from the input DW-MRI. The third dataset was obtained from a healthy human brain in realistic clinical conditions. In this case, the objective is to show that our proposal can be applied on realistic HARDI data, and that it is reasonably efficient computationally.

4.1. Synthetic data

The dataset consists of two $16 \times 16 \times 5$ synthetic phantoms, one was provided for training, and the other was provided for testing. The segmentation results are depicted in figures 1 and 2, respectively. The angle between crossing fibers in the training set (figure 1) is relatively large compared to those of the testing set (figure 2). Although the true segmentation is not available for either of the datasets, the obtained segmentation is visually correct.

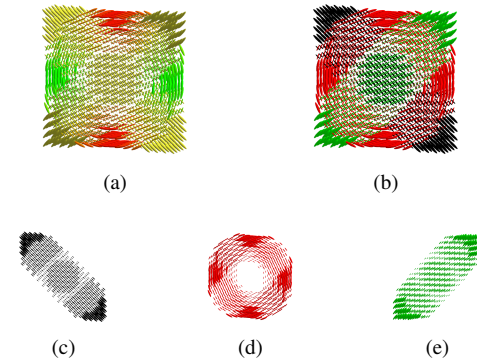


Fig. 1: MTF segmentation obtained on the phantom provided for training at the 2012 HARDI Challenge. The phantom consists of two straight- and one circular- fibers crossing at several regions. (a) Input MTF colored according to tensor orientation. (b) Segmentation obtained. (c-e) Volume segments obtained.

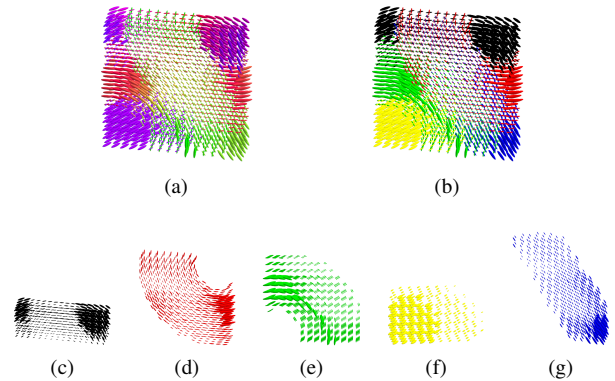


Fig. 2: MTF segmentation obtained on the phantom provided for testing at the 2012 HARDI Challenge. The phantom consists of (presumably) five fiber bundles that join in several ways. (a) Input MTF colored according to tensor orientation. (b) Segmentation obtained. (c-g) Volume segments obtained.

4.2. Phantom

The data were acquired with a 3T Tim Trio MRI system. We used the subset consisting of three 64×64 slices scanned along 64 diffusion orientations at a resolution of $3mm$, with a b-value of $1500s/mm^2$. The segmentation is depicted in figure 3. We can observe that the main difficulties occur at kissing and bifurcating bundles (green and blue in figure 3), which will likely be merged as a single bundle. Notice that this behavior is also present in Hagmann’s approach [3], since kissing and bifurcating bundles join even in POS space. However, these segments may be further processed individually by subdividing them into smaller segments or by running tractography constrained to each individual segment.

4.3. Real data

The data were acquired with a Siemens Trio 3T scanner with the following parameters: single-shot echo-planar imaging, five images with $b=1000s/mm^2$, 64 unique diffusion orienta-

²<http://www.lnao.fr/spip.php?rubrique79>

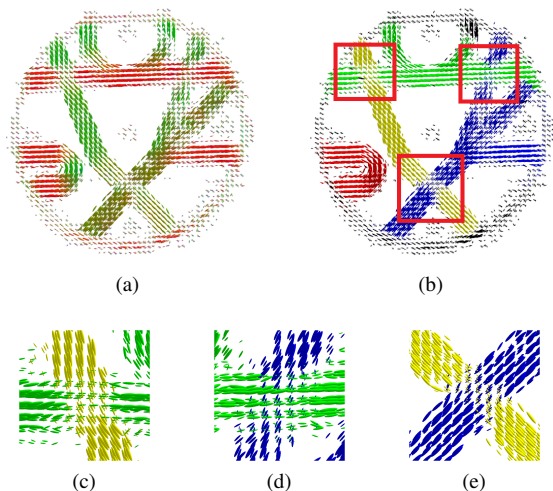


Fig. 3: MTF segmentation obtained on the fiber-cup phantom. (a) Estimated MTF colored according to tensor orientation. (b) Segmentation obtained. (c-e) Volume segments obtained.

tions, $TR = 6700ms$, $TE = 85ms$, voxel dimensions equal to $2 \times 2 \times 2mm^3$. The SNR is approximately 26. We first computed the MTF from the full dataset and then applied our segmentation algorithm to a Region of Interest (ROI) consisting of 21 central (axial) slices of the brain (approximately 30% of the data). The MTF estimation took 12 minutes and the QMMF-spectral segmentation of the ROI took 2 minutes, for a total of 14 minutes on a 1.7 GHz lap-top using one single core. In figure 4 we show the segmented MTF in input space and embedded space. In this case, we first performed a segmentation in 8 classes and then each class was subdivided in 2 subclasses, illustrating the idea that each segment may be further processed.

5. CONCLUSION

We presented a method for segmenting the cerebral white matter fiber bundles from HARDI images. We formulated the problem as a MTF segmentation problem, which allows us to handle fiber crossings. Experiments conducted on publicly available artificial datasets show that using this approach it is possible to effectively separate crossing fibers, and preliminary experiments conducted on a dataset acquired from a healthy human brain showed that the segmentation obtained is consistent with known anatomical structures.

Acknowledgments. The authors would like to thank Dr. Alonso Ramírez-Manzanares for providing us with the DW-MRI data. This research was supported in part by CONACyT grants 131369, 169178 and 131771.

6. REFERENCES

[1] H. E. Çetingül and R. Vidal. Sparse riemannian manifold clustering for hardi segmentation. In *Proc. 8th ISBI*, pages 1750–1753, 2011.

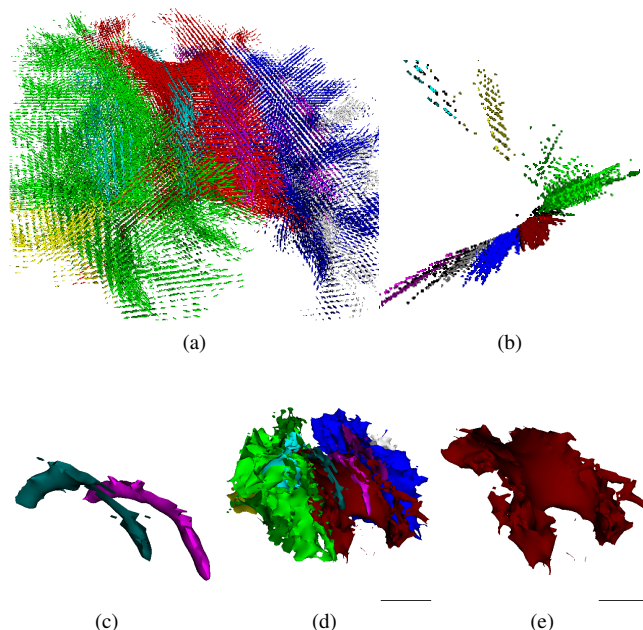


Fig. 4: Automatic segmentation obtained on 21 center axial slices from a healthy human brain. Only 14 out of 16 classes are depicted for the sake of clarity. Cingulum and corpus callosum were separated. All images are colored according to the obtained segmentation (a) MTF in input space (b) MTF embedded in \mathbb{R}^2 . (c) Cingulum bundles. (d) Segmentation iso-surfaces. (e) Corpus callosum. The iso-surfaces were smoothed out for visualization purposes.

- [2] M. Descoteaux and R. Deriche. High angular resolution diffusion MRI segmentation using region-based statistical surface evolution. *JMIV*, 33:239–252, 2009.
- [3] P. Hagmann, L. Jonasson, T. Deffieux, R. Meuli, J. Thiran, and V. Wedeen. Fibertract segmentation in position orientation space from High Angular Resolution Diffusion MRI. *Neuroimage*, 32:665–675, 2006.
- [4] L. Jonasson, P. Hagmann, X. Bresson, J. Thiran, and V. Wedeen. Representing Diffusion MRI in 5D for segmentation of white matter tracts with a level set method. In *Proc. 19th IPMI*, pages 311–320, 2005.
- [5] S. Lankton, J. Melonakos, J. Malcolm, S. Dambreville, and A. Tannenbaum. Localized statistics for DW-MRI fiber bundle segmentation. In *Proc. 21st CVPR Workshops*, pages 1–8, 2008.
- [6] K. Maschhoff and D. Sorensen. P_ARPACK: An efficient portable large scale eigenvalue package for distributed memory parallel architectures. In *3rd PARA*, pages 478–486. 1996.
- [7] M. Meila and J. Shi. Learning Segmentation by Random Walks. In *Proc. 13th NIPS*, pages 873–879, 2000.
- [8] A. Ramirez-Manzanares, M. Rivera, B. C. Vemuri, P. Carney, and T. Mareci. Diffusion basis functions decomposition for estimating white matter intravoxel fiber geometry. *IEEE TMI*, 26(8):1091–1102, 2007.
- [9] M. Rivera, O. Ocegueda, and J. L. Marroquin. Entropy-controlled quadratic markov measure field models for efficient image segmentation. *IEEE TIP*, 16(12):3047–3057, Dec. 2007.
- [10] D. Tuch, T. Reese, M. Wiegell, N. Makris, J. Belliveau, and V. Wedeen. High angular resolution diffusion imaging reveals intravoxel white matter fiber heterogeneity. *MRM*, 48(4):577–82, Oct. 2002.
- [11] D. Wassermann, L. Bloy, E. Kanterakis, R. Verma, and R. Deriche. Unsupervised white matter fiber clustering and tract probability map generation: Applications of a gaussian process framework for white matter fibers. *NeuroImage*, 51(1):228 – 241, 2010.